# SIMULTANEOUS MEASUREMENT OF EVAPORATING FUEL SPRAY USING LASER INDUCED EXCIPLEX FLUORESCENCE

**Simón Martinez-Martínez*, Fausto A. Sánchez-Cruz, Gustavo Rodríguez-Morales**

*Facultad de Ingeniería Mecánica y Eléctrica, Universidad Autónoma de Nuevo León*
*Pedro de Alba s/n, Apdo. Postal 076 Suc. F, CP. 66450, San Nicolás de los Garza, N.L., México*
*tel.: +81 83-29-40-20; fax: +81 83-32-09-04*
*simartin@gama.fime.uanl.mx*

**José M. Riesco-Ávila, Armando Gallegos-Muñoz**

*Facultad de Ingeniería Mecánica Eléctrica y Electrónica, Universidad de Guanajuato*
*Tampico Nº 912, CP. 36730, Salamanca, Guanajuato, México*
*tel.: (464) 648 0911; fax: (464) 647 2400*
*riesco@salamanca.ugto.mx*

***Abstract***

*A macroscopic analysis of experimental measurements of fuel sprays penetration on evaporating conditions using the Laser Induced Fluorescence Planar technique is presented. A pure fuel and tracers have been used to determine the two-phase process of the spray by characterizing the wavelengths they display when excited by a laser beam. An experimental set-up based on a single cylinder engine [1, 2], an Nd:YAG laser, an image acquisition system and a system of injection common rail have been used to carry out the experimental processes. Experimental results show the behaviour of the vapour phase and liquid phase in the spray under different thermodynamic conditions and injection parameters in the combustion chamber, particularly the work-fluid density and the injection pressure were observed. The measurement of these parameters is of interest to design the combustion chamber geometry and the piston bowl features of modern direct injection Diesel engines.*

*In particularly, the sschematic diagram and main components of the equipment, cross-sectional view of the cylinder head, experimental layout of PLIEF imaging tests and images, examples of the liquid phase and vapour phase penetration, maximum penetration of the liquid and vapour phase as function of the work fluid density, Maximum penetration of the phase as function of the work fluid density, maximum penetration of the liquid and vapour phase as function of the injection pressure are presented in the paper.*

***Keywords:*** *thermal engine, direct injection, liquid phase, vapour phase, penetration length*

## 1. Introduction

The key to obtain efficient combustion in modern direct injection Diesel engines is the improvement of the mixing between air and fuel. The combustion conditions are tight related to the air/fuel behaviour of the spray inside of the combustion chamber. The spray structure and its behaviour are influenced by the thermodynamic and injection parameters [1]. Along the last years, several researches have been done to identify and understand the parameters the diesel spray behaviour is related to [1-5]. Such studies have contributed with mathematical correlations [1, 3-6] or simple models for determining the spray behaviour under different conditions, and all of them are based on experimental results, where two different approaches are considered: microscopic measurements that allow to establishing the internal features of the spray, like size, distribution and drops speed; and the macroscopic measurements which are used to determine the penetration, cone angle and spray distribution.

In this work the macroscopic structure (penetration) of the fuel spray has been analyzed considering the thermodynamic parameters which usually control the spray behaviour in evaporative conditions, likewise to establish the limits that exist during the transient process of injection inside of the combustion chamber.

Basically, the experimental set-up consists of a two stokes single cylinder engine of three litres of displacement, an external equipment to control the thermodynamic variables that interact during the injection process, a laser source of Nd: YAG and an acquisition system, and an image processor.

## 2. Experimental equipment

The experimental equipment allows us to study the injection-combustion process under thermodynamic conditions (pressure, temperature and density) similar as those ones existent in actual direct injection Diesel engines at top dead centre (TDC). The main component is a single cylinder port-scavenging two-stroke engine with three-litre of displacement and low rotational speed (~500 rpm). Geometrical characteristics are presented in Table 1. The engine cycle has no net power output as injected fuel quantities are not high enough to keep the engine running, therefore, the engine needs to be motored. However, the piston compression – expansion strokes are used to obtain the realistic in-cylinder thermodynamic conditions the injection-combustion processes must be studied with.

*Tab. 1. Two stroke engine geometrical characteristics*

| | |
|---|---:|
| Bore | 150 [mm] |
| Stroke | 170 [mm] |
| Displacement | 3 [L] |
| Effective Compression Ratio | 17.1:1 |

Due to the necessity of studying the spray injection process under both inert and reacting conditions, the setup has the possibility to switch between two possible inlet atmospheres:
- Inert atmosphere, in which pure Nitrogen is supplied to the engine as intake gas due to its similarity with air. Figure 1 shows a schematic of the whole setup and the monitoring equipment for this configuration. The engine runs in a closed-loop circuit: intake Nitrogen is blown by a Roots compressor through two conditioning units and a small settling chamber into the two-stroke engine. After injection, exhaust gases (i.e., fuel and nitrogen) are cooled down and filtered by a system which separates back fuel droplets and eliminates any solid particle. The resulting clean Nitrogen is conducted back into the Roots compressor intake and the circuit is refilled with Nitrogen to compensate possible leakages.
- Reacting atmosphere, in which room air is supplied to the Roots compressor, and after compression it is conducted to the intake of the two stroke engine. Combustion gases are exhausted back to the atmosphere, as in a conventional engine. Figure 2 shows a schematic of the setup and monitoring equipment under such configuration.

The first configuration will be referred to as the ‘closed loop’ configuration, and is used to analyze the spray injection, atomization and evaporation processes, whereas the second one will be called the ‘open loop’ configuration, and is used to study the combustion process.

Our experimental results are very significant considering that they were achieved by using a quite controlled system to fill the engine cylinders based on a variable timed valve gear, without any change of the engine dimensions, compression ratio or maximum value of rotational speed.

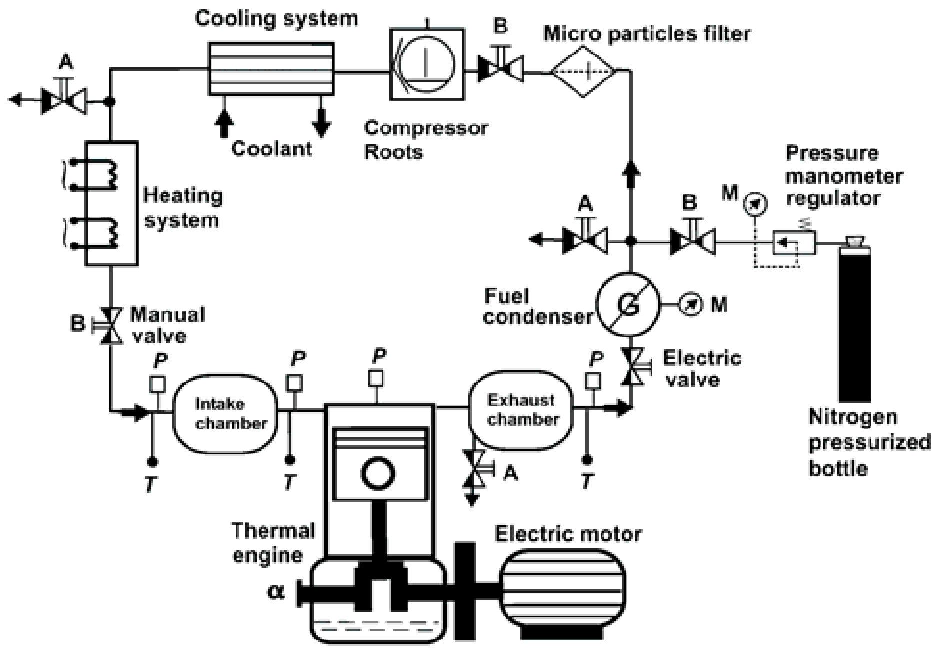


*Fig. 1. Schematic diagram and main components of the equipment running under closed-loop configuration, (i.e. the intake gas is Nitrogen)*

## Combustion Chamber Description

Figure 2 shows a schematic of the combustion chamber and the cylindrical injection chamber (45 mm diameter and 55 mm height). The injection chamber has four lateral windows, with one of them holding a pressure transducer. The injector is located on the upper wall. The 49 × 33 mm lateral windows consist of 20 mm thick quartz blocks. Details of the cylinder head can be observed in figure 3.

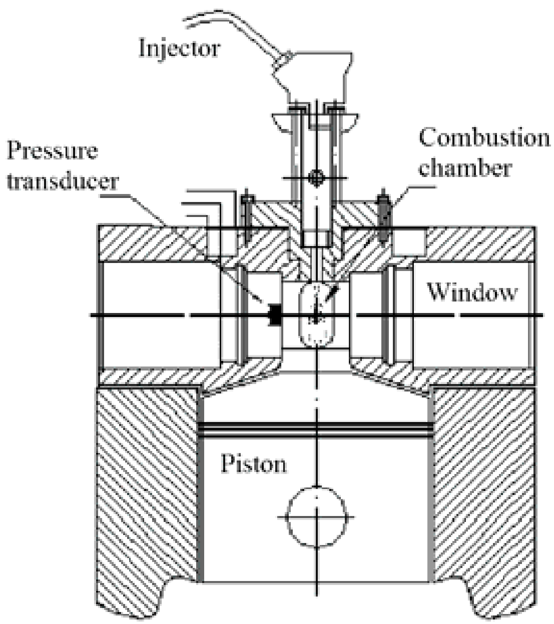


*Fig. 2. Cross-sectional view of the cylinder head*

**Injection System**

We used a Bosch common rail injection system which operates between 100 and 1800 bar. The injector uses a mini sac nozzle with a single axiallysymmetric hole, whose diameter varies from 115 to 200 μm, the last one has been used in this work. The injection system permits to vary important parameters like injection timing, pressure and frequency. The injection events last 1.5 ms. Fuel is injected every 12 cycles to keep the windows clean for better imaging.

**Engine Operating Conditions**

The engine is operated at constant speed of 500 rpm, which is optimum for testing and measurement because it minimizes lubrication and vibration issues. The quartz optical surfaces are estimated to resist up to 120 bar, and the peak cylinder pressure is kept between 60 and 80 bar. The engine block temperature is kept at a fixed temperature during all the experiments with external heater and cooler devices. An intake heater controls the intake temperatures at any value between 25 and 120 °C. Intake conditions were continuously monitored.

**Experimental Conditions**

Optical technique configuration

The laser induced exciplex fluorescence technique at the present time has extensive application in the field of the internal combustion engines, mainly in the analysis of injection processes. The laser induced exciplex fluorescence technique is based on the principle of light emission from an atom or molecule that is excited by laser radiation. Frequently, laser sources are used like illumination systems due to their monochromatically and temporally space, which gives experimental facilities superior to those of any other luminous source. Other important advantage is the excellent directionality the laser radiation has, which makes possible to construct a laser sheet through a control volume to obtain images from the radiation emitted by the fluorescence signal.

In some studies on injection processes pulsed lasers have been applied as illumination source, mainly by their short duration of radiation, which is of the order of $10^{-8}$ s, what allows to make measurements with high temporary resolution. The pulsed lasers of Nd:YAG are widely applied in the laser diagnostics. This pulsed laser uses a net crystalline of YAG (yttrium + Aluminium + deep-red) as active medium and a mixture of particles $Nd4+$. This laser is capable to produce four wavelengths and three harmonics: 1064 nm (fundamental), 532 nm (2nd harmonic), 355 nm (3rd harmonic) and 266 nm (4th harmonic) respectively.

The wavelengths more frequently used in the engineering field are: the one of 355 nm and 100 mJ, and 266 nm and 20 mJ, both with pulses of 7 ns. It is worth to mention that the energies obtained in the UV are not elevated compared with the excimero source, but there is a considerable difference of costs between the two sources of illumination, being such a difference the main disadvantages for its application. Because of the limited intensity of radiation, for the fluorescence technique intensified cameras are commonly used to gain spatial resolution, what allowed us to differentiate between both phases (liquid and vapour).

In order to study two-phase fuel spray, we considered the experimental matrix shown in Table 1, and Table 2 shows the injection conditions. When applying techniques based on fluorescence it is necessary to use special fuels, in this case the hexadecane was used, because the commercial diesel fuel presents natural fluorescent signals caused by the combination of its chemical formulation, additionally, the thermodynamic conditions where the fuel is injected causes auto-excitation of its molecules, what yield signals of fluorescence with wavelengths which interfere with the wavelengths of work for the laser beam. Whereas the chemical formulation of a pure fuel does not produce any fluorescent emission, signals of fluorescence are only produced by the exited molecules affected by the laser beam of the fuel spray. The work wavelengths normally are of 355 and 266 nm [1]. In addition, to determine the fuel penetration of the vapour and liquid phases it is necessary to include a tracer to the fuel, which once mixed emits a signal of fluorescence with different wavelength respect to that one owing to the fuel. Such effect makes possible to differentiate between both phases. In order to achieve our objective, 50 repetitions images were taken for every exposure time with intervals of 150 μs.

*Tab. 1. Experimental conditions*

| | |
|---|---|
| Fuel | Hexadecane |
| Injection time | 1-1.5 ms |
| SOI | 3º BTDC |
| Fuel pump | Piston system |
| Speed | 1430 rpm |
| Injection pressure | 300-700-1100 bar |
| Nozzle hole diameter | 150 μm |

*Tab. 2. Injection conditions*

| $P_{intake}$ [bar] | $P_{inj.}$ [bar] | $T_{intake}$ [K] | $T_{TDC}$ [K] | $P_{TDC}$ [kg/m$^3$] |
|---|---|---|---|---|
| 1.31 | 1100 | 343 | 884.50 | 22.68 |
| 1.52 | 1100 | 343 | 880.60 | 26.01 |
| 1.75 | 1100 | 343 | 884.45 | 30.35 |
| 1.30 | 700 | 343 | 883.84 | 22.53 |
| 1.53 | 700 | 343 | 881.55 | 26.37 |
| 1.75 | 700 | 343 | 883.63 | 30.24 |
| 1.31 | 300 | 343 | 880.48 | 22.50 |
| 1.55 | 300 | 343 | 882.31 | 26.77 |
| 1.75 | 300 | 343 | 884.67 | 30.31 |

**Experimental layout**

Figure 3 shows a schematic diagram of the image acquisition system used to apply the optical technique for analyzing the fuel spray. The illumination source was a laser of Nd:YAG with maximum energy of 102 mJ, wavelength of 355 nm and a pulse of 7 ns. The laser beam was directed by an articulated arm that allowed manipulating it until the optical head. The laser sheet was formed at the end of the articulated arm.

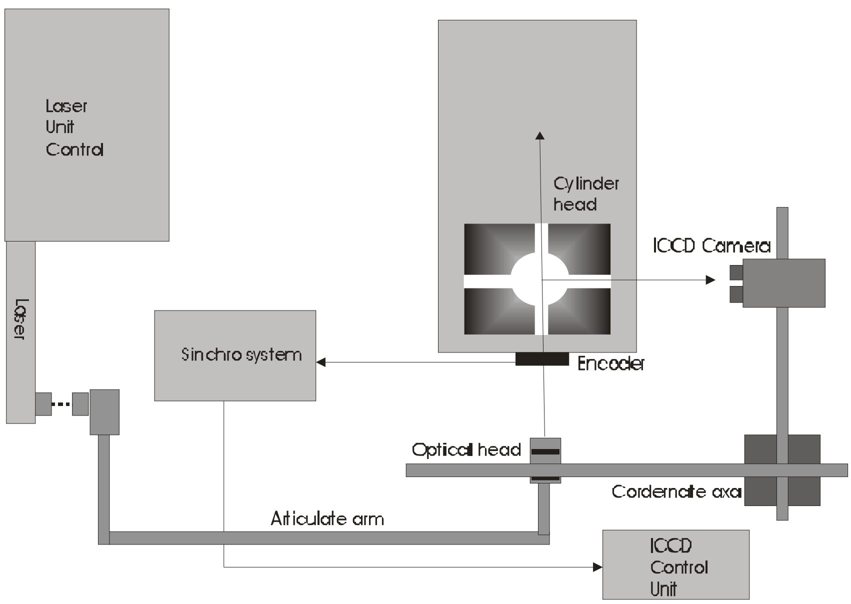


*Fig. 3. Experimental layout for PLIEF imaging tests*

The optical head consisted in three quartz lenses of high transmittance in the rank of wavelengths of the laser source, the two first lenses are spherical (fL1 = 25 mm and fL2 = 50 mm) which form a variable focus telescope, these lenses have the function to focus the beam from a distance of approximately 300 mm until$\alpha$, such focalization was only obtained by varying the distance between lenses. The third lens is a cylindrical one (fL1 = 25 mm) and its function is to form the laser sheet. By varying the distance between lenses, the change of the opening angle of the laser sheet between 20º and 40º was possible. The thickness of the laser sheet was approximately 0.5 mm, and for the experiments we used a distance work of 800 mm and an opening angle of 35º, for which the width of the sheet was 65 mm approximately. For the image acquisition an ICCD camera with a resolution of 512 x 512 pixels and a dynamic range of 16 bits was used, and an objective of 60 mm of focal length to connect an stereoscopy and an objective for the spectral range of the UV with a focal length of 100 mm, were used to take simultaneous images of the liquid and vapour phases. An exposure time of 200 ns was established, since such a time is larger than the duration period of the signal emitted by the fluorescence, which is of 50 ns, approximately.

## 3. Results

Figure 4 shows an instantaneous sequence of images taken with the PLIEF technique. A laser sheet as the main source of illumination crossed the combustion chamber. This sheet affects the fuel spray yielding certain fluorescent intensity for each phase from the molecules exitation. Such intensity is caught by the ICCD camera by means of filters of different wavelength (400 +/- 10 nm for the vapour phase and 550 +/- 10 nm for the liquid phase). For the PLIEF technique 50 images for each instant were taken, what makes a difference compared with other classical optical techniques (e.g. *ombroscopy, Schlieren, Shadowgraphy e interferometry*), which require less number of exhibition for each instant of time. The 50 images per instant in the PLIEF technique are taken to get a better spatial distribution and to attenuate phenomena associated to dispersion during the operation of the engine and the injection system. In the sequence showed in figure 4, each individual image represents the two phases, the sprays on the left hand side represents the evolution of the vapour phase, whereas the ones on the right hand side, the liquid phase. At the bottom of the images the time passed from the beginning of the injection process is indicated. The image corresponding to 150 μs shows the vapour phase and liquid phase are very similar each other, but the vapour phase is larger at the beginning, and continues growing through the combustion chamber, whereas the liquid phase remains almost constant all process long, what is observed mainly in the images between 300 and 1800 μs.

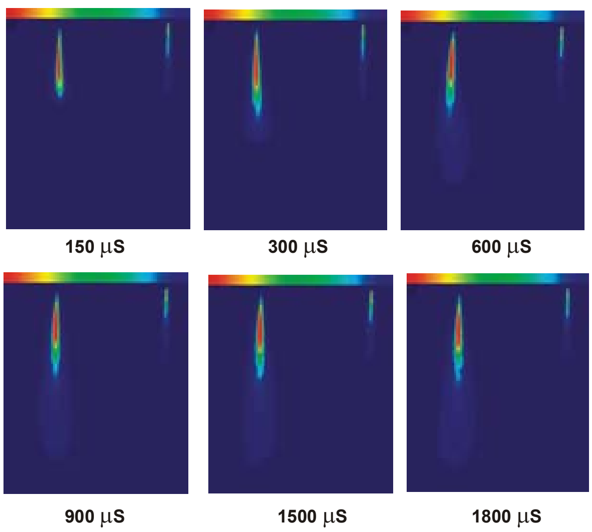


*Fig. 4. Instantaneous PLIEF images*

The optical head consisted in three quartz lenses of high transmittance in the rank of wavelengths of the laser source, the two first lenses are spherical (fL1 = 25 mm and fL2 = 50 mm) which form a variable focus telescope, these lenses have the function to focus the beam from a distance of approximately 300 mm until$\alpha$, such focalization was only obtained by varying the distance between lenses. The third lens is a cylindrical one (fL1 = 25 mm) and its function is to form the laser sheet. By varying the distance between lenses, the change of the opening angle of the laser sheet between 20º and 40º was possible. The thickness of the laser sheet was approximately 0.5 mm, and for the experiments we used a distance work of 800 mm and an opening angle of 35º, for which the width of the sheet was 65 mm approximately. For the image acquisition an ICCD camera with a resolution of 512 x 512 pixels and a dynamic range of 16 bits was used, and an objective of 60 mm of focal length to connect an stereoscopy and an objective for the spectral range of the UV with a focal length of 100 mm, were used to take simultaneous images of the liquid and vapour phases. An exposure time of 200 ns was established, since such a time is larger than the duration period of the signal emitted by the fluorescence, which is of 50 ns, approximately.

## 3. Results

Figure 4 shows an instantaneous sequence of images taken with the PLIEF technique. A laser sheet as the main source of illumination crossed the combustion chamber. This sheet affects the fuel spray yielding certain fluorescent intensity for each phase from the molecules exitation. Such intensity is caught by the ICCD camera by means of filters of different wavelength (400 +/- 10 nm for the vapour phase and 550 +/- 10 nm for the liquid phase). For the PLIEF technique 50 images for each instant were taken, what makes a difference compared with other classical optical techniques (e.g. *ombroscopy, Schlieren, Shadowgraphy e interferometry*), which require less number of exhibition for each instant of time. The 50 images per instant in the PLIEF technique are taken to get a better spatial distribution and to attenuate phenomena associated to dispersion during the operation of the engine and the injection system. In the sequence showed in figure 4, each individual image represents the two phases, the sprays on the left hand side represents the evolution of the vapour phase, whereas the ones on the right hand side, the liquid phase. At the bottom of the images the time passed from the beginning of the injection process is indicated. The image corresponding to 150 μs shows the vapour phase and liquid phase are very similar each other, but the vapour phase is larger at the beginning, and continues growing through the combustion chamber, whereas the liquid phase remains almost constant all process long, what is observed mainly in the images between 300 and 1800 μs.

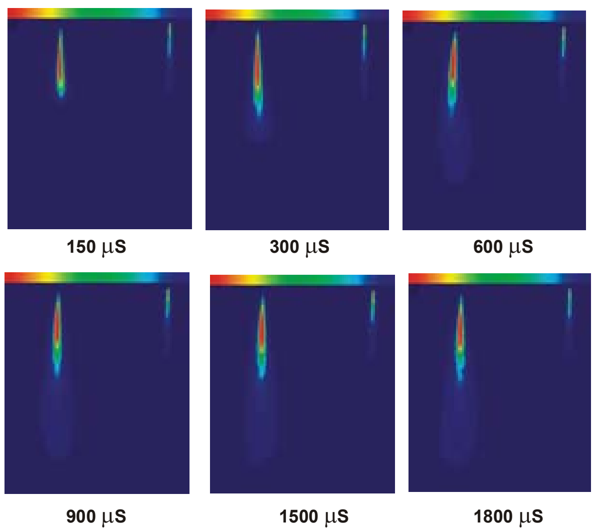


*Fig. 4. Instantaneous PLIEF images*

In equation (1) a greater energy for the vaporization of the injected fuel indicates the aerodynamic entrainment of the work fluid increases proportionally to the square root of the density of the work fluid, providing larger energy to the injected fuel.

Additionally, the effects of the density of the work fluid shown in figure 6 represent another favourable result regarding the penetration of the liquid phase, mainly for the high speed engines, which have relatively small combustion chambers and high compression ratios (of the order of 19:1), which are superior to those ones of the heavy duty engines for which the compression ratios are about 14:1, in all cases for obtaining similar pressures (up to 3 bar). This brings the result that the work fluid density is up to 40 % respect to the heavy duty engines, and therefore, this yields a shortening of the liquid phase of the spray due to the increment of the vaporization rate. An excellent profit when having high densities of the work fluid inside the combustion chamber is to avoid the impingement of the liquid phase on the piston bowl wall or in the combustion chamber, what allows reducing the pollution emissions, mainly soot and non-burned hydrocarbons. The regression and the mathematical correlation for the liquid phase and vapour phase penetration are shown in figures 6 and 7. The correlation for liquid phase penetration is $LLP = K\rho^{(-0.6595)}$, and for the vapour phase penetration, $VPP = K\rho^{(-0.2805)}$. Then, it is evident the density of the work fluid has very significant effects on the two-phase penetration of the fuel spray.

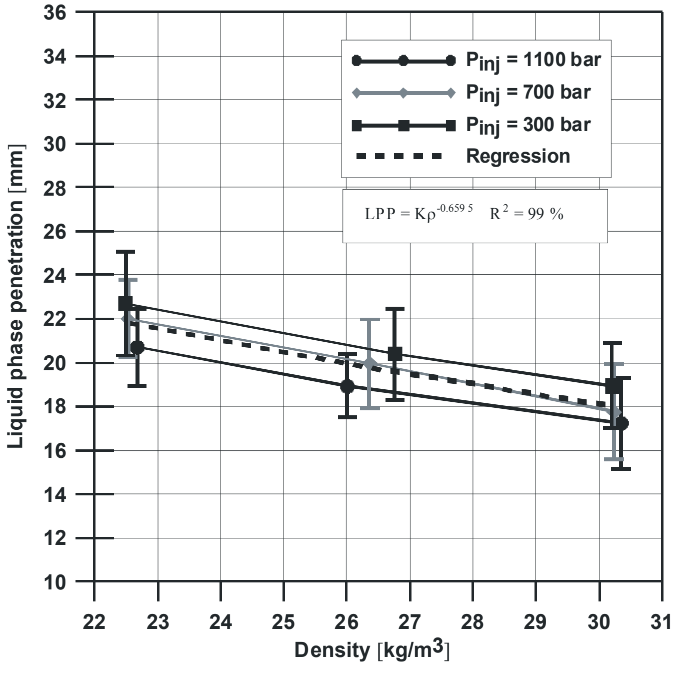


*Fig. 6. Maximum penetration of the liquid phase as function of the work fluid density: injection pressure (300, 700 and 1100 bar) and nozzle hole diameter of 200 μm*

-Liquid phase and vapour phase penetration versus the injection pressure

Figures 8 and 9 present the penetration of the liquid phase and vapour phase as functions of the injection pressure for three different densities of the work fluid. The plots show the injection pressure does not have significant effect on the experimented injection pressures ratio.

Kamimoto et al [12], Yeh et al [13], Siebers [7] and Martinez [1, 17] reported similar results, nevertheless, Kamimoto et al, and Yeh et al, carried out their experiments at very low temperatures compared to the other researches, being therefore more exact the results provided by the last ones. The shortages effects of the injection pressure on the penetration of the liquid phase indicates that the change of fuel flow, due to the increment of the injection pressure, causes an increase in the vaporization rate of the injected fuel. This also explains why the liquid length does not experience changes reaching the maxima penetration. The results show that using high injection pressures will not yield impingement on the piston bowl wall or on the combustion chamber.

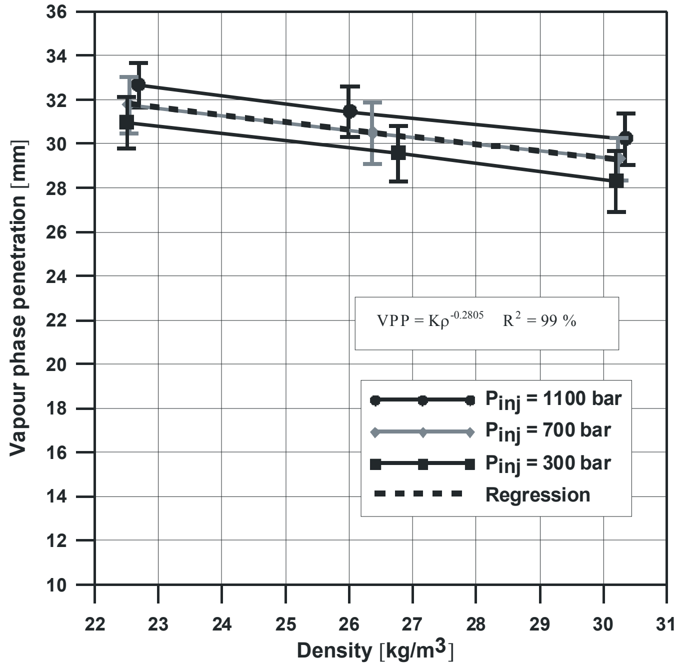


*Fig. 7. Maximum penetration of the vapour phase as function of the work fluid density: injection pressure (300, 700 and 1100 bar) and nozzle hole diameter of 200 μm*

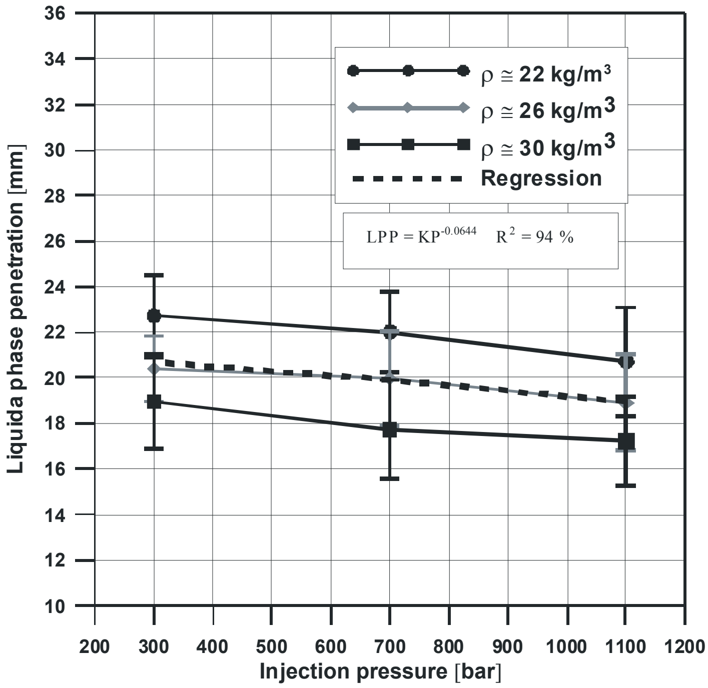


*Fig. 8. Maximum penetration of the liquid phase as function of the injection pressure: work fluid density (≅ 22, ≅ 26 and ≅ 30 kg/m³) and nozzle hole diameter of 200 μm*

According to figures 8 and 9, the dependency of the liquid phase clearly indicates the fuel vaporization is controlled by the aerodynamic entrainment (i.e. turbulent mixture process). However, it is possible to say the spray penetration behaviour is related to the control of the turbulent mixture and to the local interface process. For the case of the injection pressure, some studies have demonstrated that variations of the injection pressure does cause visible changes in the spray drops, see for instance Hodges et al. [14], Siebers [15], Desantes et al. [5] and Martinez [1, 17].

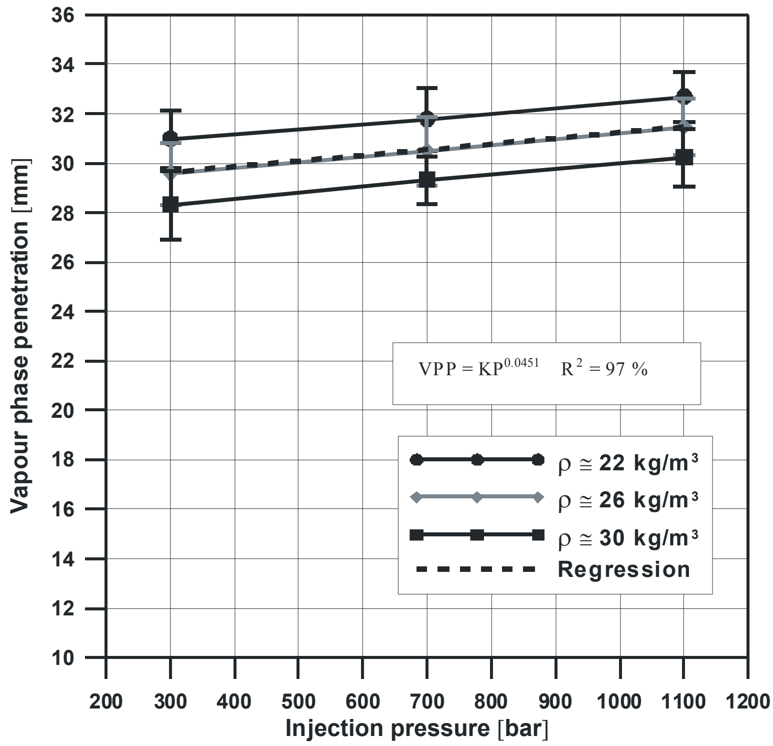


*Fig. 9. Maximum penetration of the vapour phase as function of the injection pressure: work fluid density (≅ 22, ≅ 26 and ≅ 30 kg/m$^3$) and nozzle whole diameter of 200 μm*

The main effects related to changes in the injection pressure are the heat and mass transport in the surface and the penetration of the training drops of the spray. The global effect of an increase in the injection pressure is the large penetration length before the drops evaporate; nevertheless, the life time of the drops is relatively short due to the aerodynamic entrainment during the injection process [8]. In figures 8 and 9 the dish line indicates to the regression and the correlation defining how the injection pressure affects the liquid phase and vapour phase penetration. For the penetration of the liquid phase the correlation is $LLP = KP_{inj}^{(-0.0644)}$ and for the vapour phase $VPP = KP_{inj}^{(-0.0451)}$, then the injection pressure is a not significant parameter for the maxima penetration length. In summary we can say the tendency shown in figures 8 and 9 indicates that the evaporation process is governed by the mixed process of the fuel spray, and the spray vaporization depends on the aerodynamic entrainment, this is acceptable mainly for the modern direct injection engines. The previous statement does not mean that the atomization processes and individual drops vaporization are not important [1], which these are not limited by the rate of vaporization; nevertheless, other factors may affect the local interface and transport processes. Examples of these factors may be the low volatility of fuels, the high viscosity of fuels or the low pressures of injection.

## 4. Summary and conclusions

The maximum penetration of the liquid phases and vapour phase of the fuel has been studied using Laser Inducer Excipliex Fluorescence technique. The analyzed parameters were the work fluid density and the injection pressure. The results provide a specific way to understand the effects the parameters have on the liquid phase and vapour phase penetration. Additionally, a significant understanding of processes governing the fuel vaporization phenomenon in injected sprays has been gain.

The experiments have been developed in a thermal engine with optical accesses for the combustion chamber. The injection has been carried out in an inert atmosphere to observe, by means of optical techniques, the behaviour of the spray in two-phase without the interference of

pre-ignition processes or combustions. A pure fuel was used and plotting to define both phases. The fuel and the tracers were injected by means of an injection common rail system electronically controlled.
- The work fluid density has a very significant effect on the maxima spray penetration. An increase in the work fluid density causes a reduction in the spray penetration, being greater the effect at intermediate density, and mainly in the final penetration of the liquid phase. Such a fact is consequence of a larger energy transport towards the liquid drops compared with the mixture concentration.
- The injection pressure does not have significant effects on the maxima penetration of the phases; it only causes the reduction of time to reach the maxima penetration length of the liquid phase, allowing therefore an acceleration of the aerodynamic entrainment of the vapour phase.

**Acknowledgements**

*The main support was provided by the European Community under the Energy Programme (ENK6-CT2000-00101) and CONACYT (Project 60499). The authors wish to acknowledgments the assistance and recommendations from PhD Vicente R. Bermudez and PhD José M. García, also like to thanks our colleagues and staff at the Autonomous University of Nuevo León, México.*

**References**

[1] Martínez, S., *Desarrollo de una Instalación Experimental para el Estudio de Chorros Diesel Evaporados en Atmósfera Inerte y Reactiva,* Tesis Doctoral, Valencia, España, 2003.
[2] Bermúdez, V., García, J. M., Juliá J. E. Martinez, S., *Engine with Optically Accessible Cylinder Head: A Research Tool for Injection and Combustion Processes,* SAE Technical paper 2003-1999-01, 2003.
[3] Naber, D. L., Siebers, D. L., *Effects of Gas Density and Vaporization on Penetration and Dispersion of Diesel Sprays,* SAE technical paper 960034, 1996.
[4] Siebers, D. L., *Liquid-Phase Fuel Penetration in Diesel Spray,.* SAE technical paper 980809, 1998.
[5] Desantes, J. M., Pastor, J. M., Martínez, S., Riesco, J. M., *Experimental Characterization of the Liquid Phase Penetration on Evaporating Diesel Sprays,* SAE technical paper 2005-01-2095, 2005.
[6] Bruneaux, G., Verhoeven, D., Baritaud, T., *High Pressure Diesel Spray and Combustion Visualization in a Transparent Model Diesel Engine,* SAE technical paper 1999-01-3648, 1999.
[7] Denis, L. S., *Liquid-Phase Fuel Penetration in Diesel Sprays,* SAE technical paper 980809, 1998.
[8] Browne, K. R., Partridge, I. M., Grevves, G., *Fuel Property Effects on Fuel/Air Mixing in an Experimental Diesel Engine Liquid-Phase Fuel Penetration in Diesel Sprays*. SAE technical paper 860223, 1986.
[9] Hiroyasu, H., Arai, M., *Structure of Fuel Sprays in Diesel Engines*, SAE Transaction, Vol. 99, 1990.
[10] Reitz, R. D. Bracco, F., *On the Dependence of Spray Angle and Others Sprays Parameters on Nozzle Design and Operating Conditions*, SAE technical paper 790494, 1979.
[11] Denis, L. S., *Spray Angle and Atomization in Diesel Sprays*, SAE Transaction, Vol. 93, 1984.
[12] Kamimoto, T., Yokato, H., Kobayashi, H., *Effect of High Pressure Injection on Soot Formation Processes in a Rapid Compression Machine to Simulate Diesel Flames*. SAE Transaction, Vol. 96, 1987.

[13] Yeh, C. D., Kamimoto, T., Kobori, S. Kosaka, H., *2-D Imaging of Fuel Vapor Concentration in a Diesel Spray via Exciplex-Based Fluorescence Technique*, SAE technical paper, 932652, 1993.
[14] Hodges, J. T., Baritaud, T. A., Heinze, T. A., *Planar Liquid and Gas Fuel and Droplet Size Visualization in a DI Diesel Engine*, SAE technical paper 910726, 1991.
[15] Siebers, D. L., *Scaling Liquid-Phase Fuel Penetration in Diesel Spray Based on Mixing-Limited Vaporization*, SAE technical paper 1999-01-0528, 1999.
[16] Christoph, E., Dec, J. E., *The Effect of TDC Temperature and Density on the Liquid-Phase Fuel Penetration in a D.I. Diesel Engine*, SAE technical paper 952456, 1995.
[17] Martínez, M. S., Riesco, A. J. M., Gallegos, M. A., *Phenomenological Study of the Liquid Phase Penetration on Diesel Sprays*, International Journal of KONES, 2006.